

CUTTING EDGE

Cutting Edge: The B Cell Chemokine CXC Chemokine Ligand 13/B Lymphocyte Chemoattractant Is Expressed in the High Endothelial Venules of Lymph Nodes and Peyer's Patches and Affects B Cell Trafficking Across High Endothelial Venules¹

Yukihiko Ebisuno,^{2*} Toshiyuki Tanaka,^{2*} Naotoshi Kanemitsu,^{*} Hidenobu Kanda,^{*} Kazuhito Yamaguchi,[†] Tsuneyasu Kaisho,^{‡§} Shizuo Akira,[‡] and Masayuki Miyasaka^{3*}

While CCR7 ligands direct T cell trafficking into lymph nodes (LNs) and Peyer's patches (PPs), chemokines that regulate B cell trafficking across high endothelial venules (HEVs) remain to be fully elucidated. Here we report that CXC chemokine ligand (CXCL)13 (B lymphocyte chemoattractant) is detected immunohistologically in the majority of HEVs in LNs and PPs of nonimmunized mice. Systemically administered anti-CXCL13 Ab bound to the surface of ~50% of HEVs in LNs and PPs, but not to other types of blood vessels, indicating that CXCL13 is expressed in the HEV lumen. In CXCL13-null mice, B cells rarely adhered to PP HEVs, whereas T cells did efficiently. Superfusion of CXCL13-null PPs with CXCL13 restored the luminal presentation of CXCL13 and also B cell arrest in PP HEVs at least partially. Collectively, these results indicate that CXCL13 expressed in the HEV lumen plays a crucial role in B cell trafficking into secondary lymphoid tissues such as PPs. *The Journal of Immunology*, 2003, 171: 1642–1646.

Accumulating evidence indicates that certain chemokines play a critical role in triggering the integrin-dependent adhesion of lymphocytes to high endothelial venules (HEVs)⁴ and their subsequent trafficking into lymph nodes (LNs) and Peyer's patches (PPs) (1). In particular, CC chemokine ligand (CCL)21 (secondary lymphoid tissue chemokine) and CCL19 (EBI1 ligand chemokine) are highly localized to HEVs (2, 3), and a lack of these chemokines in HEVs results in severely reduced trafficking of T cells into LNs and PPs, as seen in *plt/plt* mice, which are congenitally deficient in these

chemokines (4). Mice deficient in CCR7, the receptor for these chemokines, show a similar phenotype to the *plt/plt* mice (5).

In addition to the CCR7-mediated signaling pathway, recent studies have shown that signals through CXCR4 and CXCR5 play pivotal roles in B cell trafficking across HEVs (6). CXCR4 is signaled by CXC chemokine ligand (CXCL)12 (stromal cell-derived factor-1), whereas CXCR5 is signaled by CXCL13 (B lymphocyte chemoattractant (BLC)) that selectively attracts mature B cells as well as a small subset of T cells (7–9). Although CXCL13/CXCR5 signaling has been implicated in the migration of these cells to the follicular compartment in the spleen, LNs, PPs, and tonsils (8–10), it is not known whether CXCL13 plays any role in B cell trafficking into these tissues across HEVs.

Here we show that CXCL13 is expressed on the luminal surface of HEVs in LNs and PPs of wild-type mice. Furthermore, intravital microscopic analysis revealed that B cell arrest in PP HEVs was severely impaired in CXCL13-deficient mice, whereas T cell sticking was not affected. Upon superfusion of CXCL13-deficient PPs with CXCL13, CXCL13 was detected in the luminal surface of PP HEVs and the defect in B cell sticking was at least partially restored, indicating that CXCL13 plays a key role in the trafficking of B cells across PP HEVs.

Materials and Methods

Animals

C57BL/6 mice were purchased from SLC (Hamamatsu, Japan) and housed under specific pathogen-free conditions. CXCL13-deficient mice were generated by replacing the coding region between the 24th and 66th amino acids with the inverted neomycin resistance gene (T. Kaisho and S. Akira, unpublished observations). The CXCL13-deficient mice were backcrossed to C57BL/6 mice at least four times and used. This CXCL13-null mouse strain exhibits essentially the same phenotype as that previously reported (10). The experimental protocol

*Laboratory of Molecular and Cellular Recognition, Osaka University Graduate School of Medicine, Suita, Japan; †Institute of Laboratory Animals, Yamaguchi University School of Medicine, Ube, Japan; ‡Research Institute for Microbial Diseases, Osaka University, Suita, Japan; and §Research Center for Allergy and Immunology, The Institute of Physical and Chemical Research (RIKEN), Yokohama, Japan

Received for publication January 7, 2003. Accepted for publication June 19, 2003.

The costs of publication of this article were defrayed in part by the payment of page charges. This article must therefore be hereby marked *advertisement* in accordance with 18 U.S.C. Section 1734 solely to indicate this fact.

¹ This work was supported in part by a Grant-in-Aid and a grant for Advanced Research on Cancer from the Ministry of Education, Culture, Sports, Science and Technology of Japan.

² Y.E. and T.T. contributed equally.

³ Address correspondence and reprint requests to Dr. Masayuki Miyasaka, Laboratory of Molecular and Cellular Recognition, Osaka University Graduate School of Medicine, C8, 2-2, Yamada-oka, Suita 565-0871, Japan. E-mail address: mmiyasak@orgct.l.med.osaka-u.ac.jp

⁴ Abbreviations used in this paper: HEV, high endothelial venule; LN, lymph node; PP, Peyer's patch; PNAd, peripheral node addressin; MAdCAM-1, mucosal addressin cell adhesion molecule-1; 5-TRITC, tetramethylrhodamine-5-isothiocyanate; CCL, CC chemokine ligand; BLC, B lymphocyte chemoattractant; CXCL, CXC chemokine ligand.

was approved by the Ethics Review Committee for Animal Experimentation of Osaka University Medical School.

Antibodies

Polyclonal anti-mouse CXCL13 Abs (M-17 and V-20) were purchased from Santa Cruz Biotechnology (Santa Cruz, CA). Dot blot analysis indicated that these Abs reacted specifically with mouse CXCL13 and failed to cross-react with human and mouse CCL21, human CCL19, or human CXCL13 (data not shown). Amino acid sequencing of the immunizing peptides (Santa Cruz Biotechnology) revealed that the M-17 and V-20 Abs were raised against the mouse CXCL13 peptides KSLSSTPQAPVSKRRAA (93–109 aa) and VNPRAKWLQRLLRHVQ (76–91 aa), respectively. Biotinylated anti-mouse CCL19, anti-mouse CCL21 and anti-mouse CXCL12 Abs were obtained from DAKO (Glostrup, Denmark), PeprTech (Rocky Hill, NJ) and Santa Cruz Biotechnology, respectively. MECA-79 (anti-peripheral node addressin (PNAd)) and MECA-367 (anti-mucosal addressin cell adhesion molecule (MAdCAM)-1) were kindly provided by Dr. E. C. Butcher (Stanford University, Stanford, CA) and used as described (11, 12). Biotin-conjugated mAbs to CD3, B220, and CD11b were from BD Pharmingen (San Diego, CA).

Immunohistochemical analysis

Immunostaining of frozen sections was performed as previously described (13). Bound Abs were detected with biotinylated secondary Abs, followed by alkaline phosphatase-conjugated avidin-biotin-complex reagent (Vector Laboratories, Burlingame, CA) and Vector Red (Vector Laboratories). For double staining, the sections were further incubated with FITC- or Alexa Fluor 488 (Molecular Probes, Eugene, OR)-conjugated MECA-79 or MECA-367. To determine the proportion of chemokine-expressing HEVs, the number of HEVs positively stained with anti-chemokine Abs were counted. Approximately 100 randomly selected PNAd⁺ or MAdCAM-1⁺ HEVs were examined for each chemokine.

In situ staining analysis

Anti-CXCL13 Ab (M-17) or control goat IgG (50 µg per mouse) was administered by intracardiac injection into mice. Ten minutes after the injection, the mice were perfused with 4% paraformaldehyde, and their mesenteric LNs and PPs were harvested for the examination of Ab binding.

Intravital microscopy

Intravital microscopy was performed as described previously (14). B and T cells were isolated by incubating total splenocytes with a mixture of anti-CD3 and anti-CD11b mAbs or anti-B220 and anti-CD11b mAbs, respectively, followed by AutoMACS separation (Miltenyi Biotec, Bergisch Gladbach, Germany). The purity of the B and T cells was on average >90%, as determined by flow cytometry. The purified B and T cells were labeled with 4 µM 5-chloromethylfluorescein diacetate (Molecular Probes), and 0.8 µM tetramethylrhodamine-5-isothiocyanate (5-TRITC; Molecular Probes), respectively, for 10 min at 37°C. The fluorescently labeled B and T cells (5 × 10⁷ cells/ml) were coinjected i.v. into mice (400 µl/mouse). The behavior of the B and T cells in PPs was observed under a fluorescence microscope (BX50; Olympus, Tokyo, Japan) equipped with a CCD camera (DP50; Olympus) or a videorecorder (DCR-TRV50; Sony, Tokyo, Japan). Subsequently, Alexa Fluor 488-labeled anti-MAdCAM-1 mAb (25 µg/mouse) was injected i.v. to identify MAdCAM-1⁺ HEVs. In some experiments, PPs of CXCL13-deficient mice were perfused with mouse CXCL13 (DAKO; 50 µg/ml in PBS for 90 min) as described previously (15). QuickTime movies were generated with the Adobe Premier software.⁵

Lymphocyte migration assay

Fluorescently labeled T and B cells were coinjected i.v. into mice as above. The mice were sacrificed 6 h after injection, and the spleen and mesenteric LNs were harvested. The number of lymphocytes that had migrated into these tissues was determined by flow cytometry using an EPICS-XL flow cytometer (Beckman Coulter, Fullerton, CA). Because the cells were brightly labeled with 5-TRITC, fluorescence from 5-TRITC, which was excited by the argon laser (488-nm), was successfully detected by the photomultiplier FL2. Although a significant amount of 5-chloromethylfluorescein diacetate fluorescence was also collected by the FL2 detector, it could be easily distinguished from 5-TRITC fluorescence by the difference in intensity.

Results and Discussion

CXCL13 is expressed in the majority of HEVs

While looking for genes specifically expressed in HEVs (11, 12) we noticed that transcripts for a B cell chemokine CXCL13/BLC were found in low abundance in cDNA libraries that we generated from PNAd⁺ HEVs and MAdCAM-1⁺ HEVs. Therefore, we performed immunohistochemical analyses to examine whether CXCL13 is expressed in HEVs at the protein level. As shown in Fig. 1, the anti-peptide Ab against mouse CXCL13 (M-17) reacted strongly with MAdCAM-1⁺ LN HEVs from wild-type mice (Fig. 1, *top panels*); this reaction was almost completely abrogated by the addition of a 100-fold excess (in molar ratio) of the M-17 Ag peptide used to generate the M-17 Ab, but not by the V-20 peptide (Fig. 1, *middle panels*). Further verifying the specificity of this Ab, M-17 failed to react with any cell components in LN sections obtained from the CXCL13-deficient mice (Fig. 1, *bottom panels*). These results strongly indicate that the CXCL13 protein is expressed in MAdCAM-1⁺ LN HEVs. Furthermore, as shown in Fig. 2, the anti-CXCL13 Ab reacted with the majority of PNAd⁺ HEVs as well as MAdCAM-1⁺ HEVs in the LNs and PPs, although the extent of the reactivity was variable in different HEV segments. In addition, an anti-CCL21 Ab also reacted with over 80% of the HEVs, suggesting that both CXCL13 and CCL21 are expressed simultaneously in the majority of HEVs in these lymphoid tissues. In contrast, an anti-CCL19 Ab reacted with ~50% of the HEVs in LNs and PPs, in line with the observation in human tonsils (3). In addition, an anti-CXCL12 Ab also bound to a considerable proportion of HEVs in LNs and PPs (data not shown) as previously reported (6).

CXCL13 is apparently expressed in the luminal surface of HEVs

We next addressed whether CXCL13 is present in the luminal surface of HEVs in a form that is accessible to the receptor-bearing lymphocytes. Intracardiac injection of the anti-CXCL13 M-17 Ab yielded distinct binding to the luminal surface of

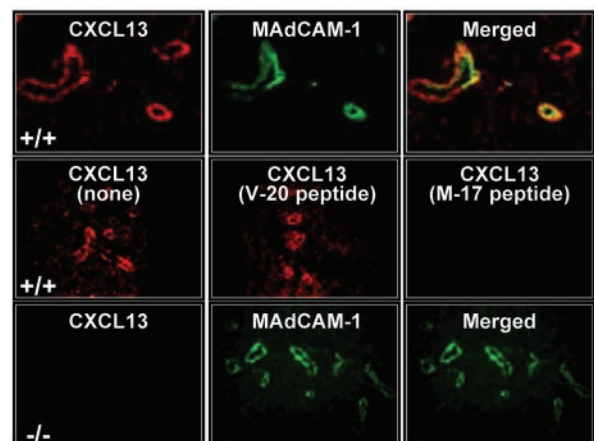


FIGURE 1. Immunohistochemical analysis of CXCL13 expression in LN HEVs. *Top panels*, Dual staining of mesenteric LNs from wild-type mice with Abs to CXCL13 (M-17) (red) and MAdCAM-1 (green). *Middle panels*, Competitive inhibition of anti-CXCL13 (M-17) binding with the M-17 peptide or irrelevant V-20 peptide. *Bottom panels*, Dual staining of mesenteric LNs from CXCL13-null mice. Sections were doubly stained with Abs to CXCL13 and MAdCAM-1 as above. Note the distinct CXCL13 staining in MAdCAM-1⁺ HEVs in the wild-type mice but the lack of such staining in CXCL13-null mice. Original magnification, ×400

⁵ The on-line version of this article contains supplemental material.

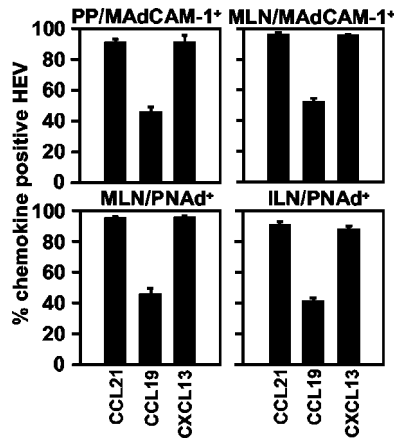


FIGURE 2. Expression of CXCL13, CCL21, and CCL19 in the HEVs of PPs and LNs. Cryostat sections of PPs, mesenteric LNs (MLN), and inguinal LNs (ILN) were incubated with an FITC-conjugated HEV-specific mAb (MECA-79 or MECA-367) and an anti-chemokine Ab as indicated, followed by a biotinylated secondary Ab and alkaline phosphatase-conjugated avidin-biotin complex. Data are represented as the percentage of chemokine-expressing HEVs (\pm SD) observed in PPs and LNs. Approximately 100 randomly selected HEVs were examined for the expression of each chemokine.

~50% of HEVs in the PPs and mesenteric LNs of wild-type mice (Fig. 3, *A* and *B*). The apparent luminal staining was observed only in typical HEV-type blood vessels of the wild-type mice, and no staining was observed in any blood vessels of the CXCL13-deficient mice (Fig. 3*C*). Injection of a control goat Ab gave no detectable staining in either of the mouse strains (data not shown). These results indicate that at least a fraction of the CXCL13 that accumulates in the HEVs was present in the luminal surface.

Despite the strong expression of the CXCL13 protein in HEVs, only low levels of CXCL13 mRNA were detected by in

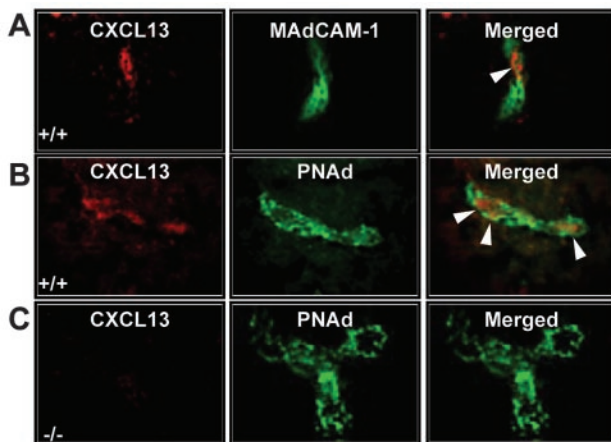


FIGURE 3. Luminal presentation of CXCL13 on the HEVs of PPs and LNs. Anti-mouse CXCL13 (M-17) was administered by intracardiac injection to wild-type mice (*A* and *B*) and CXCL13-null mice (*C*). Ten minutes after the injection, the mice were perfused with 4% paraformaldehyde, and PPs (*A*) and mesenteric LNs (*B* and *C*) were immediately removed for examination. The sections were fixed in acetone and incubated with a biotinylated secondary Ab, followed by alkaline phosphatase-conjugated avidin-biotin-complex reagent. Vector Red (red) was used as a fluorescent substrate. The sections were further incubated with Alexa Fluor 488-conjugated MECA-79 or MECA-367 (green). Arrowheads indicate anti-CXCL13 staining on the luminal surface of HEVs. Original magnification, \times 1000

situ hybridization (data not shown), suggesting that CXCL13 mRNA may be expressed by HEVs only weakly if at all. Certain chemokines such as CCL19, which is produced by nonendothelial stromal cells in lymphoid tissues, have been shown to be delivered to and presented by HEVs (3). Therefore, it is conceivable that CXCL13 protein expressed in HEVs is produced in some non-HEV region(s) within the lymphoid tissue and subsequently transported to HEVs. Follicular dendritic cells are certainly a possible source of CXCL13, because they have been shown to produce it (7). The derivation of the CXCL13 protein detected in the HEVs needs to be determined in future investigation.

B cell adhesion occurs only poorly in HEVs in CXCL13-deficient mice

We next asked whether CXCL13 is involved in B cell adhesion to HEVs. To this end, we i.v. injected into wild-type or CXCL13-deficient mice B cells and T cells that had been labeled with different fluorescent dyes and monitored the behavior of these cells within the PPs by intravital microscopy. In the wild-type mice, the injected B and T cells both showed rolling along and firm adhesion to the endothelium of HEVs in the PPs as expected (Fig. 4, *A* and *B*, *top panels*). As has been reported by Warnock et al. (16) and Miura et al. (17), some of the injected B and T cells bound differentially to distinct HEV segments. At the same time, a substantial proportion of the cells accumulated in the same HEV regions, in line with the above observation that both CCL21 and CXCL13 are expressed in the majority of HEVs. In fact, Warnock et al. (16) also described the presence of HEVs that allowed adhesion of T and B cells. In CXCL13-null mice (Fig. 4, *A* and *B*, *middle panels*), however, where HEVs were much less abundant than in wild-type controls, it was notable that B cells rolled well but adhered poorly to the HEV segments, whereas T cells rolled and arrested efficiently, as was observed in the wild-type mice. The apparently uncompromised behavior of T cells in the CXCL13-null environment was expected, given that the expression of other HEV-associated chemokines including CCL21 and CXCL12 in the HEVs of CXCL13-deficient mice was unaffected (data not shown). When short-term homing assays of purified T and B cells were performed, we found that B cells migrated into the mesenteric LNs of the CXCL13-deficient mice at a reduced level than in normal mice, whereas they migrated into the spleen of the CXCL13-deficient and wild-type mice at comparable levels (Fig. 4*C*). In contrast, coinjected T cells migrated equally well into the mesenteric LNs, as well as the spleen, in normal and CXCL13-deficient mice (Fig. 4*C*). These results are compatible with the above results obtained by intravital microscopy.

Reconstitution of CXCL13 restores B cell sticking in CXCL13-null PP HEVs

Because it may be argued that CXCL13-deficiency could induce indirect defects in B cell sticking to HEVs observed in BLC-null mice, we next investigated whether reconstitution of CXCL13 expression in CXCL13-deficient HEVs could induce B cell sticking. Upon superfusion of PPs with CXCL13, MAdCAM-1⁺ HEVs of PPs of CXCL13-deficient mice restored CXCL13 expression as evidenced by the appearance of in situ staining with anti-CXCL13 Ab (Fig. 4*D*), indicating that CXCL13 exogenously administered by superfusion was transported to the luminal surface of PP HEVs. When fluorescently labeled lymphocytes were injected i.v. subsequent to the

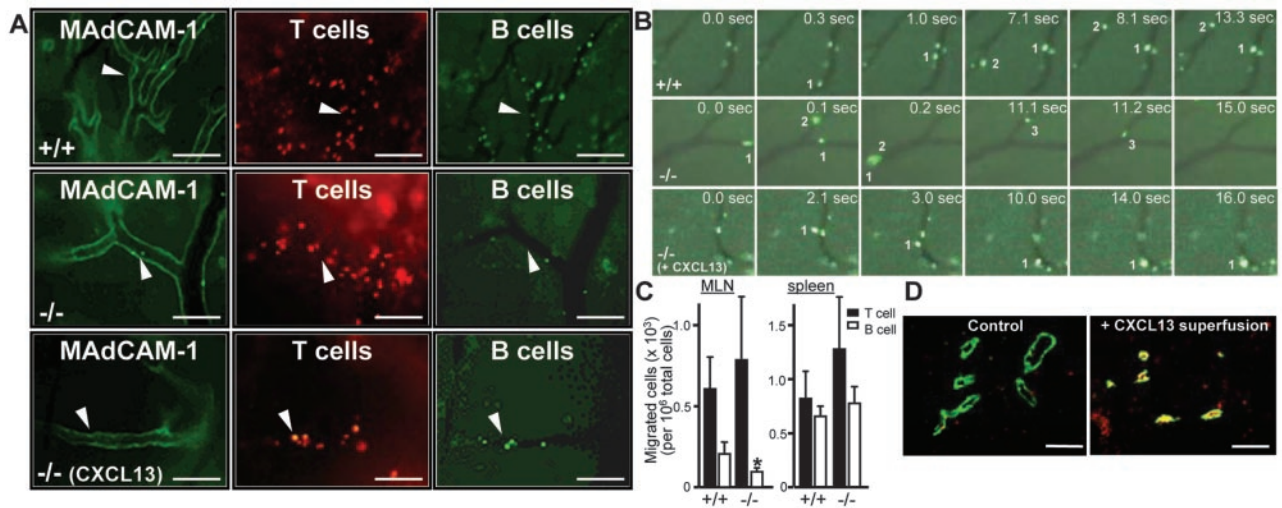


FIGURE 4. B cell accumulation in HEVs and migration into secondary lymphoid tissues in CXCL13-deficient mice. *A* and *B*, Adhesion of lymphocytes to MAdCAM-1⁺ HEVs in PPs. Fluorescently labeled lymphocytes were injected i.v. into wild-type mice (*top panels*), CXCL13-null mice (*middle panels*), and CXCL13-null mice whose PPs had been superfused with CXCL13 (*bottom panels*). *A*, The behavior of the T cells (red) and B cells (green) in the PPs was monitored. Arrowheads indicate identical positions in different panels to help align the images. *B*, Representative time-lapse intravital micrographs of PP HEVs, in which injected B cells show adhesive interactions with the HEV luminal surface. Time elapsed from the start of the recording is shown in each image. In a wild-type mouse (*top panels*), two B cells (numbered 1 and 2) that appeared in HEV at 0.3 s and 7.1 s, respectively, showed rolling, subsequently adhered to the luminal surface at 8.1 s, and remained adherent thereafter. In a CXCL13-deficient mouse (*middle panels*), all B cells entering HEV (numbered 1–3) rolled but uniformly failed to adhere to the luminal surface. In a CXCL13-null mouse of which PPs had been superfused with CXCL13 (*bottom panels*), a B cell (numbered 1) showed rolling and subsequently adhered to HEV at 10.0 s and stayed there thereafter. (For details, see supplemental movies available in the online version of this article.) *C*, Migration of B and T cells into the spleen and mesenteric LNs. B and T cells were coinjected as in *A*, and the numbers of lymphocytes that had migrated into the spleen or mesenteric LNs were counted 6 h after injection. Results shown are the number of migrated cells per 10⁶ total cells (mean ± SD). *, *p* < 0.05. *D*, Reconstitution of luminal CXCL13 presentation in PP HEVs of CXCL13-null mice. Superfusion of PPs of CXCL13-null mice with CXCL13 was performed before intravital microscopic analysis as in *A*. Mice were then given an i.v. injection of anti-CXCL13 Ab and stained as in Fig. 3. Note that the lumen of some HEVs is strongly positive for anti-CXCL13 binding. Bar, 100 μm.

CXCL13 superfusion, not only T cells but also B cells adhered to PP HEVs of CXCL13-deficient mice (Fig. 4, *A* and *B*, *bottom panels*), while B cell sticking was less abundant than that seen in wild-type mice. These results demonstrate that forced expression of CXCL13 restored B cell sticking to PP HEVs at least partially in CXCL13-deficient mice.

Our results are consistent with the observation by Okada et al. (6) that signals through CXCR5 are critically important to B cell sticking to PP HEVs. The present study also extends their finding to show that CXCL13, a physiological ligand for CXCR5, is essential for B cell adhesion to certain HEV segments in PPs. However, with regard to the LN HEVs, the CXCL13 expression and its role in B cell homing reported in the present study are at variance with the previous report by Okada et al. (6). In this regard, it should be noted that we used an anti-CXCL13 Ab (M-17) that is different from what Okada et al. used in immunohistochemical analysis. The anti-CXCL13 Ab (M-17) gave heterogeneous but significant staining in different HEVs and a different anti-CXCL13 Ab (V-20) that recognizes a different amino acid sequence from M-17 gave only faint staining in the HEVs (data not shown), possibly indicating that not all epitopes of CXCL13 in HEVs are presented equally on HEVs. Some epitopes of CXCL13 may be more readily detected than others. In addition, we examined B cell homing into mesenteric LNs at a time point that is different from what Okada et al. used; we analyzed B cell migration at 6 h after B cell injection, whereas Okada et al. investigated it at 90 min after B cell injection. These differences in the experimental conditions may, at least in part, account for the apparent discrepancy between the two studies.

In conclusion, the present investigation demonstrates that CXCL13 is expressed in the luminal surface of HEVs in LNs and PPs and plays a crucial role in B cell trafficking across HEVs. Further investigation of the mechanisms of B cell trafficking across HEVs is now warranted, which should lead to a more precise understanding of the molecular cues that guide B cells to appropriate sites.

Acknowledgments

We thank Dr. E. C. Butcher for the MECA-79 and MECA-367 mAbs. We also thank Drs. T. Murai and T. Hirata for critical reading of the manuscript, T. Kondo for technical help, and S. Yamashita and M. Komine for secretarial assistance.

References

- Kunkel, E. J., and E. C. Butcher. 2002. Chemokines and the tissue-specific migration of lymphocytes. *Immunity* 16:1.
- Gunn, M. D., K. Tangemann, C. Tam, J. G. Cyster, S. D. Rosen, and L. T. Williams. 1998. A chemokine expressed in lymphoid high endothelial venules promotes the adhesion and chemotaxis of naive T lymphocytes. *Proc. Natl. Acad. Sci. USA* 95:258.
- Baekkevold, E. S., T. Yamanaka, R. T. Palframan, H. S. Carlsen, F. P. Reinhold, U. H. von Andrian, P. Brandtzaeg, and G. Haraldsen. 2001. The CCR7 ligand ELC (CCL19) is transcytosed in high endothelial venules and mediates T cell recruitment. *J. Exp. Med.* 193:1105.
- Nakano, H., and M. D. Gunn. 2001. Gene duplications at the chemokine locus on mouse chromosome 4: multiple strain-specific haplotypes and the deletion of secondary lymphoid-organ chemokine and EBI-1 ligand chemokine genes in the *plt* mutation. *J. Immunol.* 166:361.
- Förster, R., A. Schubel, D. Breitfeld, E. Kremmer, I. Renner-Müller, E. Wolf, and M. Lipp. 1999. CCR7 coordinates the primary immune response by establishing functional microenvironments in secondary lymphoid organs. *Cell* 99:23.
- Okada T., V. N. Ngo, E. H. Ekland, R. Förster, M. Lipp, D. R. Littman, and J. G. Cyster. 2002. Chemokine requirements for B cell entry to lymph nodes and Peyer's patches. *J. Exp. Med.* 196:65.
- Gunn, M. D., V. N. Ngo, K. M. Ansel, E. H. Ekland, J. G. Cyster, and L. T. Williams. 1998. A B-cell-homing chemokine made in lymphoid follicles activates Burkitt's lymphoma receptor-1. *Nature* 391:799.

8. Schärli, P., K. Willmann, A. B. Lang, M. Lipp, P. Loetscher, and B. Moser. 2000. CXC chemokine receptor 5 expression defines follicular homing T cells with B cell helper function. *J. Exp. Med.* 192:1553.
9. Förster, R., A. E. Mattis, E. Kremmer, E. Wolf, G. Brem, and M. Lipp. 1996. A putative chemokine receptor, BLR1, directs B cell migration to defined lymphoid organs and specific anatomic compartments of the spleen. *Cell* 87:1037.
10. Ansel, K. M., V. N. Ngo, P. L. Hyman, S. A. Luther, R. Förster, J. D. Sedgwick, J. L. Browning, M. Lipp, and J. G. Cyster. 2000. A chemokine-driven positive feedback loop organizes lymphoid follicles. *Nature* 406:309.
11. Izawa, D., T. Tanaka, K. Saito, H. Ogihara, T. Usui, S. Kawamoto, K. Matsubara, K. Okubo, and M. Miyasaka. 1999. Expression profile of active genes in mouse lymph node high endothelial cells. *Int. Immunol.* 11:1989.
12. Saito, K., T. Tanaka, H. Kanda, Y. Ebisuno, D. Izawa, S. Kawamoto, K. Okubo, and M. Miyasaka. 2002. Gene expression profiling of mucosal addressin cell adhesion molecule-1⁺ high endothelial venule cells (HEV) and identification of a leucine-rich HEV glycoprotein as a HEV marker. *J. Immunol.* 168:1050.
13. Ezaki, T., L. Yao, and K. Matsuno. 1995. The identification of proliferating cell nuclear antigen (PCNA) on rat tissue cryosections and its application to double immunostaining with other markers. *Arch. Histol. Cytol.* 58:103.
14. Yamaguchi, K., and G. I. Schoeffl. 1983. Blood vessels of the Peyer's patch in the mouse. II. In vivo observations. *Anat. Rec.* 206:403.
15. Hickey, M. J., M. Forster, D. Mitchell, J. Kaur, C. De Caigny, and P. Kubes. 2000. L-selectin facilitates emigration and extravascular locomotion of leukocytes during acute inflammatory responses in vivo. *J. Immunol.* 165:7164.
16. Warnock, R. A., J. J. Campbell, M. E. Dorf, A. Matsuzawa, L. M. McEvoy, and E. C. Butcher. 2000. The role of chemokines in the microenvironmental control of T versus B cell arrest in Peyer's patch high endothelial venules. *J. Exp. Med.* 191:77.
17. Miura, S., Y. Tsuzuki, D. Fukumura, H. Serizawa, M. Suematsu, I. Kurose, H. Imaeda, H. Kimura, H. Nagata, M. Tsuchiya, and H. Ishii. 1995. Intravital demonstration of sequential migration process of lymphocyte subpopulations in rat Peyer's patches. *Gastroenterology* 109:1113.